Research Article

Identification of CXCR4 Upregulation in Diffuse Large B-Cell Lymphoma Associated with Prognostic Significance and Clinicopathological Characteristics

Yi-an Zhang [iD],[1] **Xue Yang** [iD],[1] **Jiamei Yao** [iD],[2] **Yuhong Ren** [iD],[1] **and Peng Liu** [iD][1,3]

[1]*Department of Hematology, Zhongshan Hospital, Fudan University, Shanghai, China*
[2]*Department of Pathology, Zhongshan Hospital, Fudan University, Shanghai, China*
[3]*Cancer Center, Zhongshan Hospital, Fudan University, Shanghai, China*

Correspondence should be addressed to Peng Liu; liu.peng@zs-hospital.sh.cn

Yi-an Zhang, Xue Yang, and Jiamei Yao contributed equally to this work.

Background. Diffuse large B-cell lymphoma (DLBCL) is a heterogeneous malignant lymphoma with distinct characteristics. Patients with treatment failure after the standard immunochemotherapy have worse prognosis, which implies the necessity to uncover novel targets. The C-X-C chemokine receptor 4 (CXCR4) overexpression has been identified in several hematopoietic malignancies. However, the expression signatures and prognostic significance of CXCR4 in DLBCL associated with clinicopathological features remain unclear. *Methods.* Gene expression profiles of DLBCL were obtained from the Cancer Genome Atlas (TCGA) and Gene Expression Omnibus (GEO) databases. Then, a meta-analysis with an integrated bioinformatic analysis was performed to assess the relationship between CXCR4 expression and clinicopathological features of DLBCL. Finally, experimental verification including immunohistochemical (IHC) staining and real-time quantitative PCR (qPCR) was carried out using patient samples. In vitro cell line viability tests were conducted using CXCR4 inhibitor WZ811. *Results.* DLBCL patients with activated B-cell-like (ABC) subtype have higher expression level of CXCR4 with worse survival. Differential expressed genes in the CXCR4-upregulation group were enriched in canonical pathways associated with oncogenesis. DLBCL with CXCR4 upregulation had lower degree of CD8$^+$ T cell infiltration. TIMER analysis demonstrated that the CXCR4 expression was positively correlated with the expression of CD5, MYC, NOTCH1, PDCD1, CD274, mTOR, FOXO1, and hnRNPA2B1 in DLBCL. IHC study in patient samples showed the positive correlation between CXCR4 and nongerminal center B-cell (non-GCB) subtype and mTOR expression. Meanwhile, quantitative polymerase chain reaction results revealed that high CXCR4 mRNA level was correlated to double-hit DLBCL. Finally, cell viability test showed that WZ811 exerted antiproliferation effect in DLBCL cell lines in a dose-dependent manner. *Conclusion.* CXCR4 was upregulated in ABC-DLBCL associated with worse prognosis. Our analysis predicted CXCR4 as a potential target for DLBCL treatment, which may serve as an inhibitor both on BCR signaling and nuclear export warranting further investigation in clinical trials.

1. Introduction

Diffuse large B-cell lymphoma (DLBCL) is one of the most common types of non-Hodgkin lymphoma (NHL), which is considered aggressive but potentially curable. Despite 60% patients can be cured with the standard immunochemotherapy of R-CHOP (rituximab plus cyclophosphamide, doxorubicin, vincristine and prednisolone), those with treat-ment failure after R-CHOP often have worse outcomes [1]. With the advance in second-generation sequencing to uncover novel molecular biomarkers and signaling pathways, there is a trend toward using XR-CHOP treatment, namely, adding new drugs to the standard R-CHOP regimen. For instance, bortezomib, lenalidomide, ibrutinib, BCL2, and EZH2 inhibitors, as well as inhibitors of PI3K/AKT/mTOR, have now being used as first-line therapy in combination with

R-CHOP in patients with estimated poor prognosis according to pathological subtypes in several biomarker-driven clinical studies [2]. Nevertheless, there is limited evidence that DLBCL patients benefit more from XR-CHOP than R-CHOP [3, 4]. Therefore, further research on the genetics and pathogenesis of DLBCL is needed to identify novel molecular targets and therapeutic vulnerabilities.

Chemokines and their receptors play an important role in oncogenesis, progression, and dissemination of tumor cells [5]. CXCR4 is a chemokine receptor involved in a series of biological processes including hematopoeisis and immune response, which is highly expressed in a variety of hematological malignancies [6]. CXCR4 is a prognostic biomarker in lots of cancer diseases such as gastrointestinal cancer [7], breast cancer [8], and lung cancer [9] [10, 11]. Recent studies revealed that the CXCR4 and its ligand CXCL12 are linked to the pathogenesis of lymphohematopoietic malignancies [12, 13]. The CXCR4 expression was reported to be associated with poor prognosis, and the inhibition of CXCR4 renders tumor cells more sensitive to chemotherapy [14].

To date, there has been no consensus on the correlation between the prognostic significance of CXCR4 and clinicopathological characteristics of DLBCL. In a large cohort (training/validation cohort of 468/275), the increased expression of CXCR4 was associated with the activated B-cell-like (ABC) subtype in patients with newly diagnosed DLBCL. However, it was also an independent risk factor for progression-free survival (PFS) in germinal center B-cell-like- (GCB-) DLBCL [15]. In another study by et al., CXCR4 was not associated with the prognosis of DLBCL patients [16]. Differed results seem controversial, and an integrated analysis is lacking. In this study, we used a meta-analysis and an integrated bioinformatics analysis to conduct a comprehensive assessment of the relationship between CXCR4 expression and DLBCL. Results were further verified by immunohistochemical (IHC) staining on tissue samples from independent cohorts with in vitro cell function tests.

2. Materials and Methods

2.1. Data Mining and Clinical Samples. We searched DLBCL gene expression datasets from the Cancer Genome Atlas (TCGA) database (https://portal.gdc.cancer.gov/) and the Gene Expression Omnibus (GEO) database (https://www.ncbi.nlm.nih.gov/geo/). By using "DLBCL" or "diffuselargeBcell lymphoma," "homo sapiens," and "expression profiling" as qualifiers, we searched and screened "microarray" and "RNA sequencing" data from the year 2006-2018 in the GEO database. The inclusion criteria were as follows: detectable CXCR4 expression level, available clinicopathological data, number of datasets larger than 30 patients, and tissue samples. The diagnosis and classification of DLBCL cases were based on the criteria of the 2008 World Health Organization classification of the lymphoid neoplasms. Two independent validation cohorts, one is tissue microarray including forty-four de novo DLBCL patients, another is formalin-fixed paraffin-embedded (FFPE) samples of 59 de novo DLBCL patients, were both obtained from Zhong-

shan Hospital, Fudan University. This study was approved by the Institutional Review Board (IRB) of Zhongshan Hospital Affiliated to Fudan University (B2021-025R) and was conducted in accordance with the principles of the Declaration of Helsinki. Written informed consent was signed by each participant.

2.2. Integrated Bioinformatic Analysis. Databases from GPL570 (GSE11318, GSE23501, GSE19246, GSE31312, GSE53786, GSE64555, GSE56313, GSE74266, and GSE93986) were selected for gene set enrichment analysis (GSEA), protein-protein interaction (PPI) network, and immune cell infiltration (ICI) analysis. Subjects were categorized into low and high expression groups according to their median CXCR4 expression level. Normalization was performed, and batch effects were eliminated using the "SVA" and "limma R" packages (version3.12, http://www.bioconductor.org), and an adjusted $P < 0.05$ was selected as the threshold for enriched terms. Genes with |log 2FC (fold change) >2 were considered differentially expressed. To explore the key signal pathway differences between the CXCR4 high and low expression population, genes were characterized using the GSEA 4.1.0 software (https://www.broadinstitute.org/gsea/). Datasets c2.all.v7.2.-symbols.gmt (C2: curated gene sets) and c5.all.v7.2.symbols.gmt (C5: ontology gene sets) were obtained from the MsigDB database on the GSEA website (http://www.gsea-msigdb.org/), and the number of permutations was set at 1000. The gene sets were normalized using an enrichment score of >1, with $P < 0.05$. A false discovery rate (FDR) in GSEA of <0.25 was considered as significant enrichment gene set and was used as the standard for distinguishing significant enrichment signaling pathways. The protein-protein interaction (PPI) network was analyzed using the STRING website (http://string.embl.de/). Pathway analysis of 30 hub genes was further analyzed using the online tool KOBAS 3.0 (http://kobas.cbi.pku.edu.cn/kobas3).

2.3. ICI Level and Tumor Immune Estimate Resource (TIMER) Analysis. The CIBERSORT algorithm was performed to evaluate ICI in DLBCL tissues between CXCR4 high and low expression group. This algorithm transforms the normalized gene expression matrix into the composition of infiltrating immune cells. Analysis of ICI level between CXCR4 high and low expression groups was conducted by the "CIBERSORT R" package. Then, samples selected with a CIBERSORT P value <0.05 was filtered and reserved for the following analysis. We also used online tool TIMER2.0 (http://timer.cistrome.org/) to conduct Kaplan-Meier analysis to explore the infiltration of various immune cell subsets in patient survival from the TCGA database. Then, we used the TCGA database to explore how the CXCR4 expression was correlated with the expression of biomarkers that showed significance in the GSEA analysis.

2.4. Immunohistochemistry and Evaluation Criterion. An independent cohort of 44 de novo DLBCL tissue microarrays from Zhongshan Hospital was stained with eight antibodies. IHC staining was performed on the Leica platform

(Bond Max) according to the antibody manual (Table S1) and manufacturer's instructions. IHC was assessed by two pathologists independently. They reexamined the immunostained slides to reach a consensus when there were inconsistencies. The percentage of positive CXCR4 stained cell area was scored into four grades: 0 for none; 1, <25%; 2, 25% to 50%; 3, 50% to 75%; and 4, >75%. The intensity was as follows: 0, negative; 1, weakly staining; 2, moderately staining; and 3, strongly staining. The final immunoreactivity scores were obtained by multiplying the percentage and the intensity score (0 to 12), and a final score lower than 2 was defined as CXCR4 negative, while a score ≥ 2 represented CXCR4 positivity.

2.5. Real-Time Quantitative Polymerase Chain Reaction(qPCR).
Five 5 μm unstained FFPE tissue sections were freshly cut for gene expression analysis. Total RNA was extracted using an FFPE Total RNA Isolation Kit (Canhelp Genomics Co., Ltd., Hangzhou, China) according to the protocols. For each specimen, reverse transcription was performed on isolated total RNA using the High-Capacity cDNA Reverse Transcription Kit with RNase Inhibitor (Applied Biosystems, Foster City, CA, USA). Next, the real-time PCR (RT-PCR) reaction was applied on the 7500 Real-Time PCR system (Applied Biosystems, Japan) for analyzing gene expression profiles. The RT-PCR program was initiated at 95°C for 10 minutes, followed by 40 cycles at 95°C for 15 seconds, and 60°C for 1 minute. The mRNA quantity of specific genes, calculated using the $2^{-\triangle\triangle CT}$ method, was normalized against GAPDH. All the measurements were performed in triplicate. The sequences of the CXCR4 primer pairs were as follows: CXCR4-F: 5′-GGTG GTCTATGTTGGCGTCT-3′, CXCR4-R: 5′-TGGAGT GTGACAGCTTGGAG-3′.

2.6. In Vitro Proliferation Assay.
The effects of CXCR4 inhibitor WZ811 (MedChemExpress) were investigated by a Cell Counting Kit-8 (CCK-8; Dojindo, Kumamoto, Japan) assay. Human DLBCL cell line OCI-Ly3 (ABC type) and SU-DHL4 (GCB type) were purchased from Fuheng Cell Center, Shanghai. For time-dependent assay, tumor cells were plated in a 96-well plate, and the cell density was depended on cultured time. For dose-dependent assay, tumor cells were plated at a density of 3000 cells with different concentrations of WZ811. All assays were performed in quadruplicate. At 0 h, 2 h, and 24 h, the cell proliferation assay was performed according to the manufacturer's instructions. Absorbance was measured at a wavelength of 450 nm using a microplate reader (Flexstation III ROM V2.1.28, USA).

2.7. Statistical Analysis.
Stata 14.2 (StataCorp, TX, USA) software was applied to conduct meta-analysis. Correlations between clinicopathological features and gene protein expression were determined using a X^2 test. Study heterogeneity was accessed by a X^2 test based on the Q statistical test. We also applied a sensitivity analysis to evaluate the stability of the pooled results. Univariate and multivariate Cox regression analyses were performed using R software (ver-

sion 4.0.4). The effects of the CXCR4 expression on OS and PFS in DLBCL were analyzed using Kaplan-Meier analysis. The nonparametric Spearman r correlation coefficient was employed to assess the correlations between CXCR4 and other biomarkers. Cell viability test was analyzed using one-way ANOVA, and $P < 0.05$ was considered statistically significant.

3. Results

3.1. Correlations between CXCR4 Expression and DLBCL Subtypes Associated with Prognosis by Meta-Analysis.
Information available for 2515 patients derived from 20 datasets were included in meta-analysis. The TCGA database (workflow type: RNASeq-FPKM) included 46 DLBCL cases with CXCR4 expression values and clinical characteristics (including gender, age, clinical stage, and survival). Nineteen datasets in the GEO database (experiment type: expression profiling by array) were included, with 15 datasets available for DLBCL subtypes and 10 datasets available for survival information (Table 1). No heterogeneity was found across the datasets ($I^2 = 12.1\%$, $P = 0.321$).

14 datasets were analyzed available for DLBCL subtypes. Pooled results indicated that 5he CXCR4 expression was significantly higher in ABC subtype than in GCB subtype of DLBCL (odds ratio [OR] = 0.80, 95% CI: 0.65 to 0.99, $P = 0.039$) (Figure 1(a)). 10 datasets were analyzed available for survival data including overall survival (OS) and progression-free survival (PFS). The random effect model ($I^2 = 0.0\%$, $P = 0.518$) was used, and the pooled results indicated that the CXCR4 overexpression in DLBCL patients was related to poorer OS (HR = 1.22, 95% CI: 1.10 to 1.35, $P < 0.001$) (Figure 1(b)). After each exclusion, the impact on the combined data is small. The combined effect (random effect model, $I^2 = 0.0\%$, $P = 0.523$) showed that the CXCR4 expression in patients with DLBCL had no significant influence on PFS (HR = 1.14, 95% CI: 0.992 to1.307, $P = 0.065$) (Figure 1(c)). However, patients with higher CXCR4 expression tended to have poorer PFS.

To further clarify whether CXCR4 is an independent risk factor for DLBCL, we conducted univariate and multivariate analyses. Multivariate analysis result indicated that CXCR4 acts as an independent factor in the prediction of prognosis in DLBCL patients (Figure 1(d)). In the integrated analysis of survival (Figure 1(e)), a trend of association between CXCR4 high expression and unfavorable OS was found in DLBCLABC type ($P < 0.001$) but not GCB type ($P = 0.252$), and no association between CXCR4 high expression and unfavorable PFS for both types was found ($P > 0.05$).

3.2. Gene Enrichment Analysis Related to CXCR4 Expression by GSEA and PPI Network.
Subjects were categorized into low and high expression groups according to median CXCR4 expression level. Gene Ontology (GO) analysis showed that differential expression genes (DEGs) in subjects with higher CXCR4 expression were enriched in biological process (BP): regulation of RNA splicing, epigenetic modification, and mRNA export from the nucleus, etc.; cellular

TABLE 1: Information of the included GEO datasets.

	Year	GEO accession	Platform	Country	Patient number	Clinicopathological parameters
1	2006	GSE4732	GPL3706	USA	216	Subtype, gender, age, stage, OS
2	2008	GSE11318	GPL570	USA	172	Subtype, gender, age, stage, OS
3	2009	GSE16920	GPL7015	Japan	46	Gender, age
4	2010	GSE23501	GPL570	USA	69	Subtype, gender, age, OS, PFS
5	2010	GSE19246	GPL570	USA	59	Subtype
6	2011	GSE22470	GPL96	Germany	271	Subtype, gender, age
7	2012	GSE31312	GPL570	USA	498	Subtype
8	2012	GSE32918	GPL8432	UK	172	Subtype, gender, age, OS
9	2012	GSE38202	GPL8432	South Korea	164	Gender, age
10	2013	GSE53786	GPL570	USA	119	Subtype, gender, age, stage, OS
11	2013	GSE44164	GPL96	Germany	32	Subtype, gender, age
12	2014	GSE64555	GPL570	UK	40	Subtype
13	2014	GSE57612	GPL96	Germany	37	Subtype, gender, age, stage, OS
14	2015	GSE69051	GPL14951	UK	160	Age, OS
15	2015	GSE69049	GLP8432	UK	32	Age, OS
16	2015	GSE56313	GPL570	Denmark	55	Subtype
17	2016	GSE74266	GPL570	Denmark	62	Subtype
18	2017	GSE93986	GPL570	USA	88	Subtype, PFS
19	2017	GSE87371	GPL570	France	223	Age, gender, stage, PFS, OS

Abbreviations: GEO: Gene Expression Omnibus; OS: overall survival; PFS: progression-free survival.

component (CC): histone deacetylase complex, high-density lipoprotein particle, etc.; and molecular function (MF): methylated histone binding, insulin receptor binding, etc. (Figures 2(a)–2(c)). Analysis of C2 curated gene sets (Table S2) exhibited that these genes were significantly enriched in signaling pathways such as the JNK-MAPK pathway, PI3K-AKT, mTOR signaling pathway, B-cell receptor (BCR) pathway, B-cell poor survival, IL-2 STAT5, IL-2 PI3k pathway, and NOTCH1 signal pathway. And genes had higher transcriptional activity of smad2/3/4 heterotrimer, adipogenesis, insulin resistance, VH rearrangement, doxorubicin resistance and alkylating resistance, CD5 target up, MYC and TFRC-up, and TP53 expression and degradation (Figure 2(d)). However, no gene sets were significantly enriched in the CXCR4 low group at FDR < 25%.

Based on the STRING database (https://string-db.org/), the PPI network of CXCR4 was constructed with a minimum required interaction score of 0.9. We selected 30 hub genes (C3, CCR7, AURKB, CDC45, CDC6, GNG7, S1PR1, CENPM, CX3CR1, EXO1, KIF4A, MCM10, ADRA2A, CCL21, CNR1, CXCL13, DRD4, GPR183, HRAS, PNOC, FOXM1, HJURP, SYK, CDT1, SELL, UQCR10, CDCA5, HIST1H2BD, HNRNPA2B1, HNRNPH1) as center nodes of the interaction network (Figure 2(e)). These hub genes were further analyzed using the online tool KOBAS 3.0 (http://kobas.cbi.pku.edu.cn/kobas3) to verify the results of GSEA (Figure 2(f)).

3.3. ICI and Gene Correlation Analysis by TIMER2.0. The CIBERSORT algorithm was used to calculate the proportion of immune cells in 816 samples from databases of GPL570

(GSE11318, GSE23501, GSE19246, GSE31312, GSE53786, GSE64555, GSE56313, GSE74266, and GSE93986). We found that high CXCR4 expression tumor tissues harbored a higher level of naive B-cells ($P < 0.01$), naive CD4+ T cells ($P < 0.01$), resting memory CD4+ T cells ($P < 0.05$), and regulatory T cells (Tregs) ($P < 0.05$), while low CXCR4 expression group harbored a higher level of CD8+ T cells ($P < 0.05$), macrophage 1 ($P < 0.001$), macrophage 2 ($P < 0.01$), and resting dendritic cells ($P < 0.05$) than high expression ones (Figure 3(a)). The TIME2.0 website integrates a series of algorithms with TCGA database or the tumor expression data submitted by users themselves to estimate specific immune cell types. The run results are more reliable, and the results are displayed visually after a comprehensive evaluation through complex calculation methods. We used Kaplan-Meier plots to explore the relationship between ICI and DLBCL prognosis (CIBERSORT analytic module). We found that CD8 + T cell ($P = 0.0355$) infiltration was significantly correlated with DLBCL prognosis. There was no significant correlation between prognosis and macrophage 1 and macrophage 2 infiltration (Figure 3(b)). Based on the above GSEA and PPI results, we assessed the relationship between CXCR4 expression level and the expression of MYC, PDCD1(PD-1), CD274(PD-L1), Notch1, mTOR, CD5, FOXO1, and hnRNPA2 gene markers that showed significance in the GSEA analysis above using TIMER 2.0 (TCGA database). The results showed that the expression of CXCR4 was positively correlated with the expression of these genes (Figure 3(c)).

3.4. IHC Validation of CXCR4 Expression in DLBCL Patient Samples Associated with Clinicopathological Features. Tissue
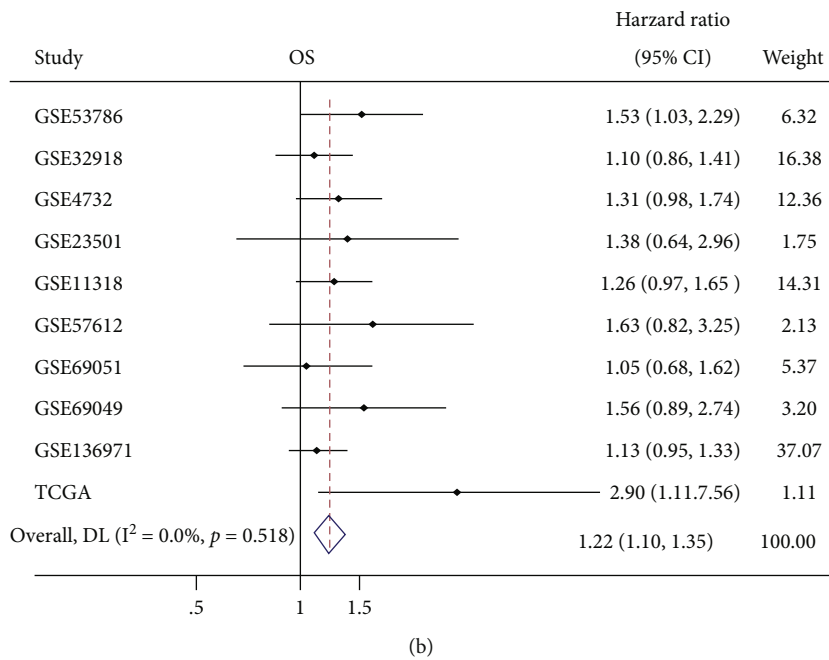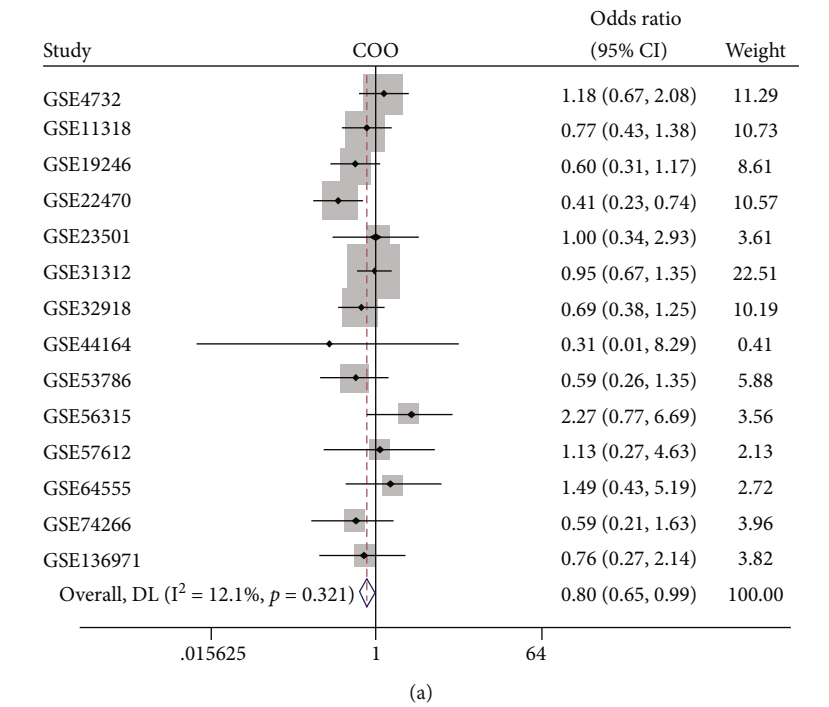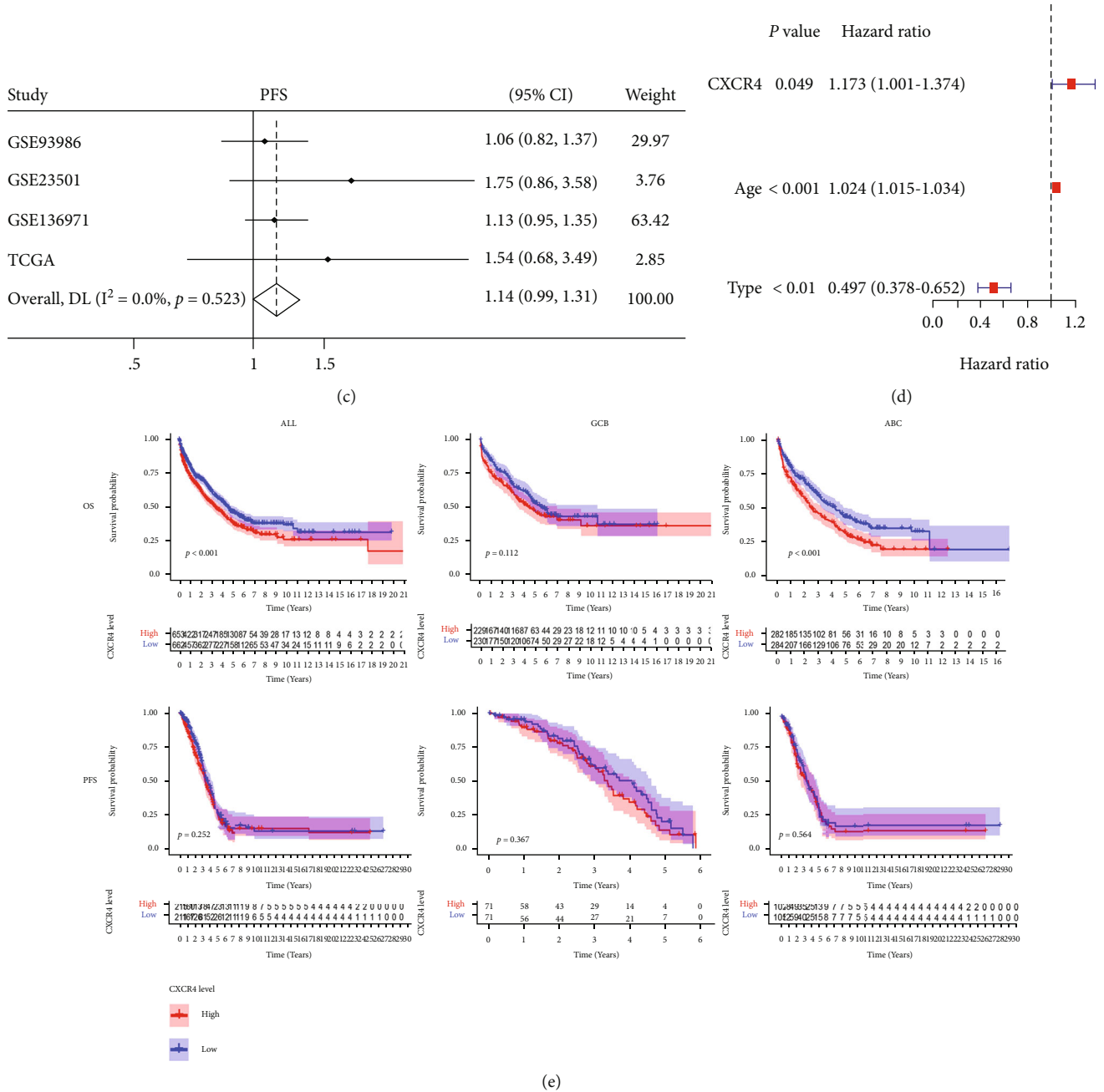
(a)

(b)

Figure 1: Continued.

(c)

(d)

(e)

FIGURE 1: Forest plots of the (a) CXCR4 expression and cell of origin subtypes in DLBCL. (b) The CXCR4 expression and overall survival in DLBCL. (c) Progression-free survival. (d) Multivariate cox proportional hazards regression analysis. (e) Integrated analysis of the CXCR4 expression on overall survival (upper) and progression-free survival (lower) in DLBCL analyzed by Kaplan–Meier plot curves. Abbreviations: COO: cell of origin; overall survival: OS; progression-free survival: PFS; GCB: germinal center B-cell-like; ABC: activated B-cell-like.

microarrays of 44 de novo DLBCL were examined by IHC, including 26 men and 18 women with a median age of 60 years (range, 29-82 years). Thirteen (29.5%) samples were positive for CXCR4, which were stained dark or light brown, and distributed in the membrane and cytoplasm of lymphoma cells (Figures 4(a)–4(c)). The clinicopathological features of the patients and their relationship with CXCR4 protein expression are summarized in Table 2. No association was identified between the expression of CXCR4 and age, gender, Ann Arbor stage, and IPI score ($P > 0.05$). The

protein expression level of CXCR4 was found to be positively associated with the cell of origin (COO) of the non-GCB subtype ($P = 0.022$), and with high levels of the mTOR expression (Figures 4(d)–4(f)). No correlation was found between the expression level of CXCR4 and CD8 + T lymphocyte infiltration, c-MYC, tp53, and PD-1 and PD-L1 expression.

Further, to verify the mRNA level of CXCR4 in DLBCL and its correlation to clinical characteristics, another independent cohort of 59 de novo DLBCL patients, all
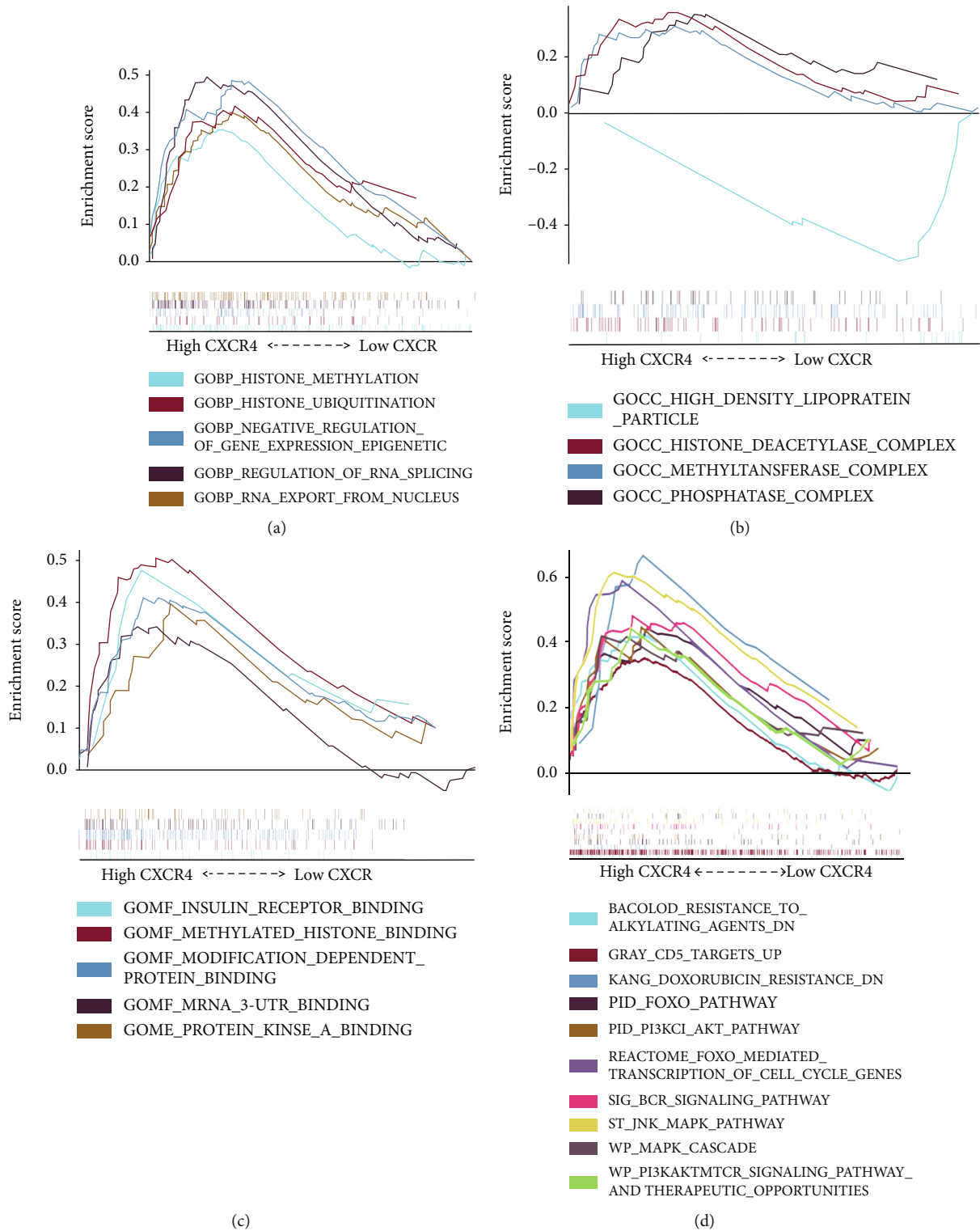
(a)

(b)

(c)

(d)

Figure 2: Continued.

(e)

Hub gene	Counts
C3	20
CCR7	17
AURKB	16
CDC45	14
CDC6	14
GNG7	14
S1PR1	14
CENPM	13
CX3CR1	13
EXO1	13
KIF4A	13
MCM10	13
ADRA2A	17
CCL21	12
CNR1	12
CXCL13	12
DRD4	12
GPR183	12
HRAS	12
PNOC	12
FOXM1	11
HJURP	11
SYK	11
CDT1	10
SELL	10
UQCR10	10
CDCA5	9
HIST1H2BD	9
HNRNPA2B1	9
HNRNPH1	9

GO enrichment

G protein-coupled receptor signaling pathway (GO:0007186)
Nucleoplasm (GO:0005654)
Dendritic cell chemotaxis (GO:0002407)
Protein binding (GO:0005515)
Immune response (GO:0006955)
Chemotaxis (GO:0006935)
DNA replication (GO:0006260)
DNA replication checkpoint (GO:0000076)
G protein-coupled receptor activity (GO:0004930)
Cell chemotaxis (GO:0060326)
Leukocyte chemotaxis (GO:0030595)
External side of plasma membrane (GO:0009897)
DNA replication origin binding (GO:0003688)
Chemokine binding (GO:0019956)
C-C chemokine receptor activity (GO:0016493)
C-C chemokine binding (GO:0019957)
G1/S transition of mitotic cell cycle (GO:0000082)
Regulation of transcription involved in G1/S transition of mitotic cell cycle (GO:0000083)
DNA replication initiation (GO:0000083)
Plasma membrane (GO:0005886)

KEGG enrichment

Chemokine signaling pathway (hsa04062)
Viral protein interaction with cytokine and cytokine receptor (hsa04061)
Cytokine-cytokine receptor interaction (hsa04060)
Neuroactive ligand-receptor interaction (hsa04080)
Kaposi sarcoma-associated herpesvirus infection (hsa05167)
Viral carcinogenesis (hsa05203)
Thermogenesis (hsa04714)
Alcoholism (hsa05034)
Human immunodeficiency virus 1 infection (hsa05170)
Human cytomegalovirus infection (hsa05163)
Fc epsilon RI signaling pathway (hsa04664)
B cell receptor signaling pathway (hsa04662)
Cardiac muscle contraction (hsa04260)
NF-kappa B signaling pathway (hsa04064)
PI3K-Akt signaling pathway (hsa04151)
C-type lectin receptor signaling pathway (hsa04625)
Sphingolipid signaling pathway (hsa04071)
Serotonergic synapse (hsa04726)
Cholinergic synapse (hsa04725)
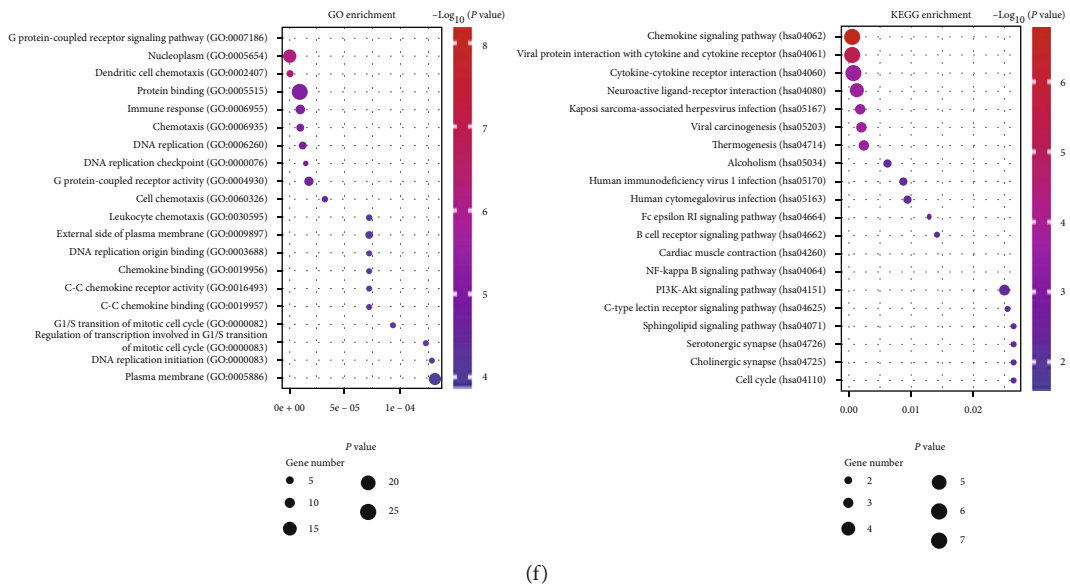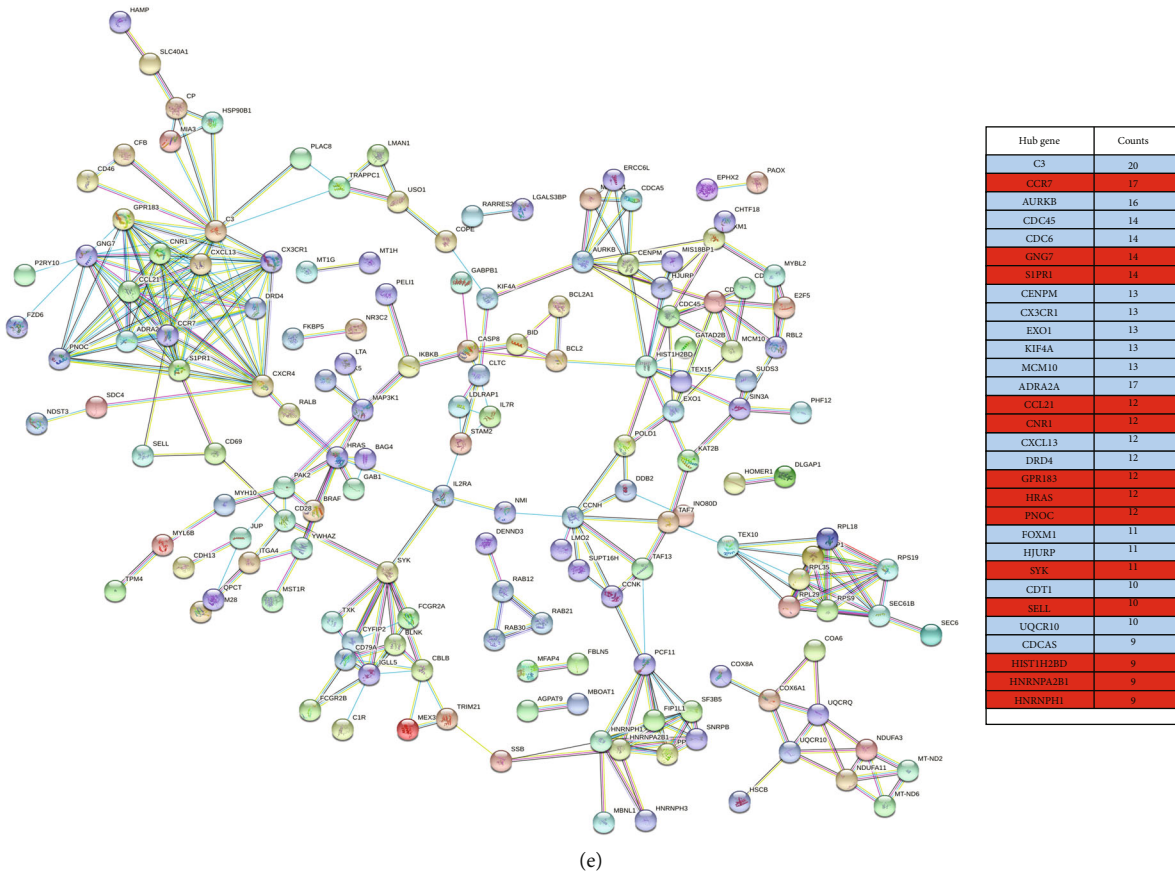Cell cycle (hsa04110)

(f)

Figure 2: GSEA Gene Ontology (GO) analysis showed that CXCR4-related genes were enriched in (a) biological process (BP), (b) cellular component (cc), and (c) molecular function (MF). (d) GSEA C2 curated gene sets analysis. (e) Protein-protein interaction network of CXCR4 by the STRING website (left). Selected 30 hub genes (C3, CCR7, AURKB, CDC45, CDC6, GNG7, S1PR1, CENPM, CX3CR1, EXO1, KIF4A, MCM10, ADRA2A, CCL21, CNR1, CXCL13, DRD4, GPR183, HRAS, PNOC, FOXM1, HJURP, SYK, CDT1, SELL UQCR10, CDCA5, HIST1H2BD, HNRNPA2B1, HNRNPH1) as center nodes of the interaction network are shown in the right table (red: upregulation; blue: downregulation). (f) GO and KEGG analysis of 30 hub genes by KOBAS 3.0.

diagnosed within 2 years and with complete treatment information, was applied for qPCR using their FFPE samples. Based on the qPCR results, high CXCR4 mRNA level was correlated to double-hit DLBCL ($P = 0.0175$)

(Figure 4(g)). However, no correlation was found between the mRNA level of CXCR4 and double-expression DLBCL and Bruton's tyrosine kinase (BTK) inhibitor or lenalidomide treatment response.
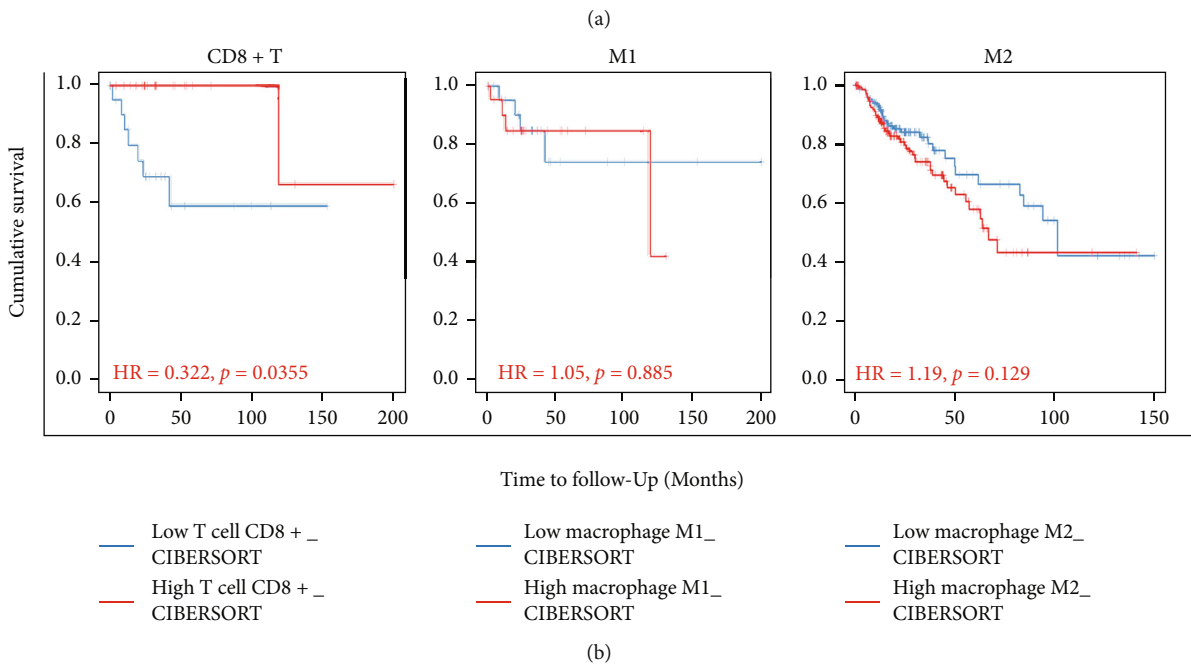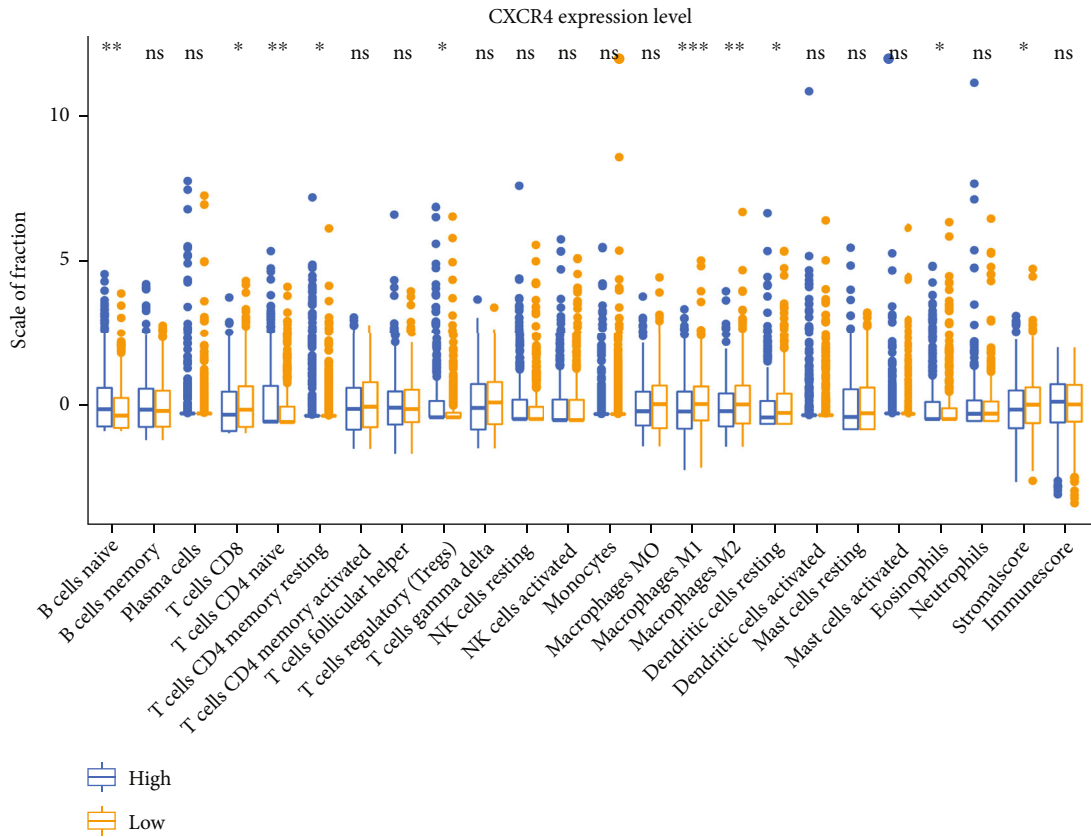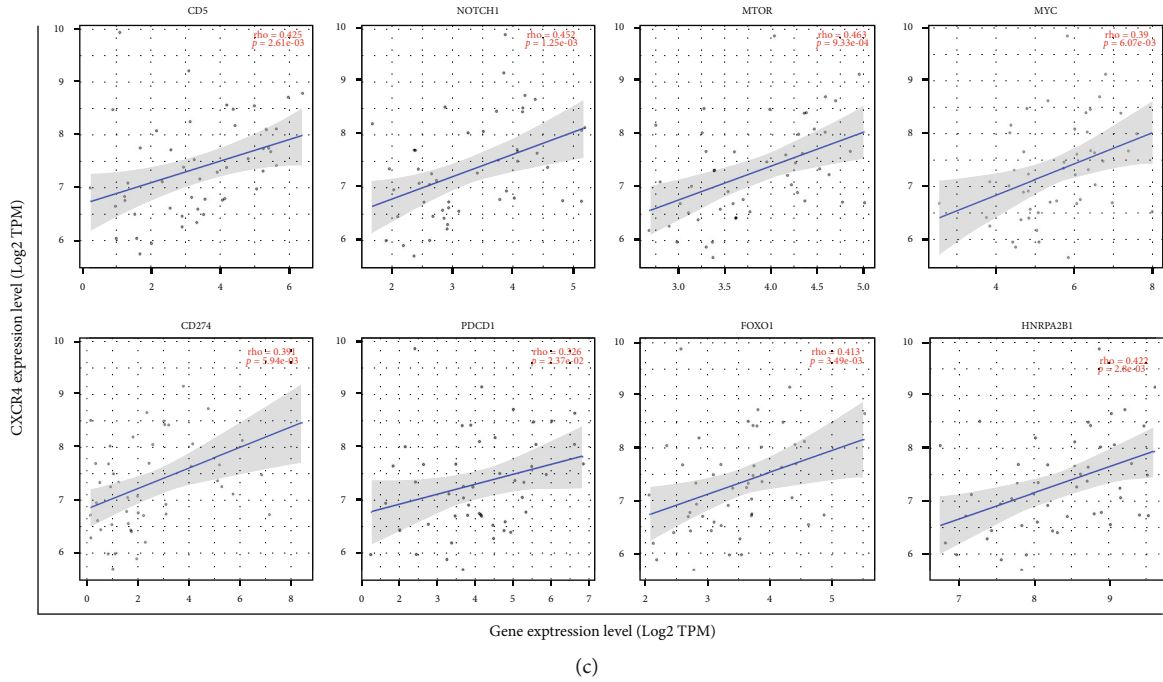
(a)

(b)

FIGURE 3: Continued.

(c)

FIGURE 3: Immune cell infiltration and gene correlation analysis. (a) Immunocyte infiltration levels of 22 types of immune cells between high and low CXCR4 expression groups. (b) Relationship between degree of immune cell CD8 + T cell (left), macrophage 1 (middle) and macrophage 2 (right) infiltration, and DLBCL prognosis (CIBERSORT analytic module) by Kaplan-Meier plots (based on TCGA database). (c) TIMER2.0 analysis of gene correlation between CXCR4 and CD5, Notch1, MTOR, MYC, PDCD1 (PD-1), CD274 (PD-L1), FOXO1, and hnRNPA2B1.
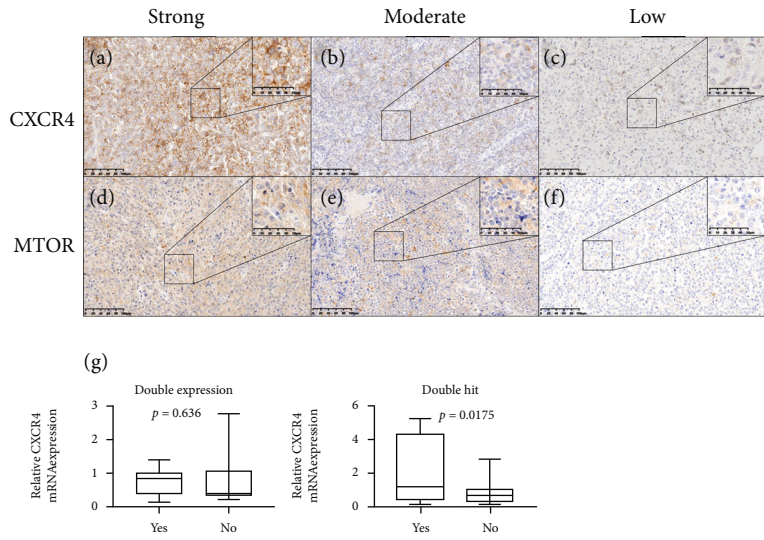

FIGURE 4: Representative photomicrographs (original magnification: ×200; upper right corner, ×400) of CXCR4 and MTOR immunohistochemical staining in DLBCL tissues. (a) Strongly positive expression status, (b) moderately positive expression status, and (c) weakly positive expression status of CXCR4 in DLBCL tissues. (d) Strongly positive expression status, (e) moderately positive expression status, and (f) weakly positive expression status of MTOR in DLBCL tissues. (g) Correlation between mRNA level of CXCR4 in DLBCL and prognostic characteristics of double expression (left) and double hit (right). High CXCR4 mRNA level was associated with double-hit DLBCL ($P = 0.0175$).

3.5. Growth Inhibition Effect of CXCR4 Inhibitor WZ811 on DLBCL Cell Lines. With the escalation of drug concentration (10, 20, 40, 80 μM), WZ811 inhibited the proliferation of DLBCL cell lines in a dose-dependent manner (Tables 3 and 4). OCI-ly3 cells exhibited more sensitivity to WZ811 treatment than SU-DHL4 cells within the range <80 μM (Figure 5). However, according to IC50 results, with the escalation of WZ811 concentration, SU-DHL4 cells exhibited

TABLE 2: Relationship between CXCR4 expression status and clinicopathological features in DLBCL.

		CXCR4 negative	CXCR4 positive	P value
Age	<60	16	5	0.426
	≥60	15	8	
Gender	Male	17	9	0.376
	Female	14	4	
Ann Arbor stage	I-II	17	5	0.322
	III-IV	14	8	
COO	GCB	25	6	0.022
	Non-GCB	6	7	
IPI score	0-1	9	3	0.686
	≥2	22	10	
MTOR	<20%	21	4	0.024
	≥20%	10	9	
CD5	<50%	20	9	0.763
	≥50%	11	4	
CD8 + T cell infiltration	<20%	14	8	0.322
	≥20%	17	5	
C-MYC	<50%	15	8	0.426
	≥50%	16	5	
TP53	<50%	21	6	0.180
	≥50%	10	7	
PD-1	≤1%	4	3	0.404
	>1%	27	10	
PD-L1	≤1%	22	10	0.686
	>1%	9	3	

Abbreviations: COO: cell of origin.

TABLE 3: Cell viability of OCI-Ly3 and SU-DHL4 treated with WZ811.

WZ811 concentration (μM)		Cell viability %		
OCI-Ly3	0 (group 1)	100	100	100
	10 (group 2)	79.99	86.18	83.95
	20 (group 3)	77.87	76.81	72.07
	40 (group 4)	68.54	68.69	70.56
	80 (group 5)	67.45	67.62	66.15
SU-DHL4	0 (group 6)	100	100	100
	10 (group 7)	98.75	91.94	98.8
	20 (group 8)	83.47	88.53	84.29
	40 (group 9)	73.31	78.82	75.12
	80 (group 10)	61.4	63.52	68.27

more sensitivity to WZ811 treatment than OCI-Ly3 cells with a 50% inhibitory concentration (IC50) of 372.2 μM for OCI-Ly3 and 143.5 μM for SU-DHL4. Analysis results of IC50 were achieved by CompuSyn software (Version 1.0). With the prolongation of treatment time, no statistical significance was found between 0 h, 2 h, and 24 h (data not shown).

4. Discussion

Although the standard immunochemotherapy of R-CHOP has cured a majority of patients with DLBCL, treatment failure after R-CHOP still remains an intractable problem due to worse outcomes, which further underlines the importance of finding novel targets. Alizadeh et al. established the COO classification of DLBCL by using cDNA microarrays for gene expression profiling (GEP): the GCB and ABC subtype [17]. DLBCL patients with ABC subtype showed significantly worse prognosis compared with those with GCB subtype [18]. In our meta-analysis, CXCR4 was highly expressed in DLBCL patients with the ABC subtype and this was related to poor OS (Figures 1(a) and 1(b)). Our GSEA results revealed that the tumorigenicity of CXCR4 in DLBCL is related to the PI3K/AKT/mitogen-activated protein kinase (MAPK) pathways, mTOR, JNK-MAPK signal transducer and activator of transcription (STAT) pathways, Smad2/3/4, NOTCH1, and WNT signal pathways (Figure 2(d)) [19, 20]. PI3K/AKT/mTOR pathway involved in crucial functions such as cellular proliferation, cell cycle regulation, and cell motility in DLBCL [21]. JAK-STAT signaling pathways were associated with pathogenesis of ABC-DLBCL [22]. DLBCL patients with the NOTCH1 mutations have worse PFS and OS [23]. These results are consistent with

TABLE 4: Statistical results of cell viability test.

| Bonferroni's multiple comparison test		P value
OCI-Ly3	Group 2 vs. group 1	$P < 0.0001$
	Group 3 vs. group 1	$P < 0.0001$
	Group 4 vs. group 1	$P < 0.0001$
	Group 5 vs. group 1	$P < 0.0001$
	Group 3 vs. group 2	NS
	Group 4 vs. group 2	$P < 0.0001$
	Group 5 vs. group 2	$P < 0.0001$
	Group 4 vs. group 3	NS
	Group 5 vs. group 3	$P < 0.05$
	Group 5 vs. group 4	NS
	Group 6 vs. group 7	NS
	Group 6 vs. group 8	$P < 0.0001$
	Group 6 vs. group 9	$P < 0.0001$
	Group 6 vs. group 10	$P < 0.0001$
SU-DHL4	Group 7 vs. group 8	$P < 0.001$
	Group 7 vs. group 9	$P < 0.0001$
	Group 7 vs. group 10	$P < 0.0001$
	Group 8 vs. group 9	$P < 0.005$
	Group 8 vs. group 10	$P < 0.0001$
	Group 9 vs. group 10	$P < 0.001$
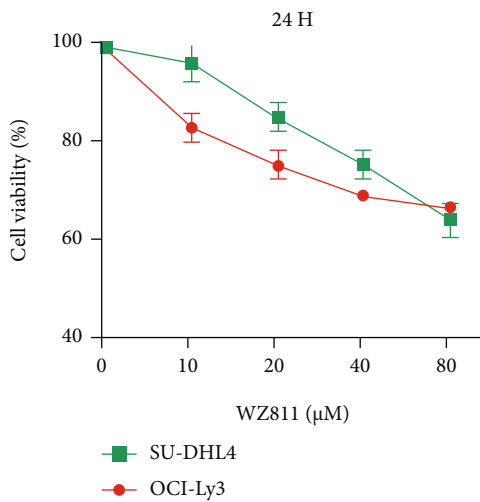
FIGURE 5: WZ811 inhibited the proliferation of the cell lines in a dose-dependent manner. DLBCL cells (OCI-Ly3 and SU-DHL4) were treated with indicated concentrations of WZ811 (0, 10, 20, 40, 80 μM) for 24 h, and cell viability was measured by cell counting kit-8 assay.

previous studies showing that the CXCR4/CXCL12 axis can mediate tumorigenicity by activating various intracellular signaling transduction pathways and downstream effectors [24–28]. Gene correlation analysis (TIMER) demonstrated that the CXCR4 expression is positively related to the degra-

dation of tumor suppressor geneTP53, upregulation of the protooncogene C-MYC, and CD5expression (Figure 3(c)). CD5$^+$ DLBCL has a poor prognosis and is classified as ABC-DLBCL with elusive genetic features [29]. This confirmed the role of CXCR4 in the ABC but not the GCB subtype of DLBCL, suggesting that CXCR4 exerts an adverse effect on the prognosis of the ABC subtype DLBCL through the above molecular signaling pathways. According to the study of Breinholt et al. [30], large B-cell lymphoma patient samples with significantly higher prevalence of MYC-BCL2-double-hit showed significantly lower expression of PD-L1 and tumor-associated macrophages. Meanwhile, our qPCR analysis showed that the high CXCR4 expression correlated to molecular cytogenetic abnormality of double-hit DLBCL (Figure 4(g)). The intrinsic relationship between CXCR4 and double-hit DLBCL deserves worth further research. However, we did not find correlations between the protein expression level of CXCR4 and CD8$^+$T lymphocyte infiltration, CD5, c-MYC, tp53, and PD-1 and PD-L1 expression. This discrepancy may due to the limited sample size of the IHC cohort.

Immune cells in the tumor microenvironment contribute to tumor progression and the antitumor responses. Their biological significance in DLBCL varies from different studies. CD8$^+$ T lymphocytes and M1 macrophage play an important role in antitumor immune responses. Our results showed that the low CXCR4 expression group harbored a higher level of CD8$^+$ T cells ($P < 0.05$) (Figure 3(a)) and M1 macrophage ($P < 0.001$) (Figure S1), which may explain a better survival result of low CXCR4 expression group. One study assessed the safety, efficacy, and immunobiological effects of the CXCR4 antagonist (BL-8040, motixafortide) combined with a PD-1 inhibitor and chemotherapy in metastatic pancreatic ductal adenocarcinoma (PDAC) [10]. CXCR4 blockade promotes CD8$^+$ effector T cell tumor infiltration and is synergistic with PD-1 inhibitors in PDAC mouse models. This study is in line with our study results. Besides, the high CXCR4 expression in DLBCL harbored a higher level of regulatory T cells (Tregs) ($P < 0.05$). It is known that Tregs are important modulators for the interaction between lymphoma cells and tumor microenvironment. Zhou [31] reported that a high infiltration of FOXP3/CTLA-4 double-positive cells was significantly associated with poor prognosis. Chang [32] found that higher infiltration of intr-tumoral CD25$^+$ FOXP3$^+$ lymphocytes correlate with a favorable prognosis in patients with DLBCL. Previous studies on the biological significance of immune cells infiltration in DLBCL [33, 34] are inconsistent. This may be due to the sample size and different materials (peripheral blood, tissue, and bone marrow) and methods (immunohistochemistry, flow cytometry, and sequencing). The effects of ICI in DLBCL on the development of DLBCL need to be verified by more fundamental experiments.

According to our GSEA results, CXCR4 coexpression genes are enriched during metabolism biological processes of adipogenesis and insulin resistance (Table S2). Recently, numerous studies have underlined the role of cholesterol metabolism in the tumorigenesis. Cholesterol metabolism regulates oncogenic signaling pathways, including the
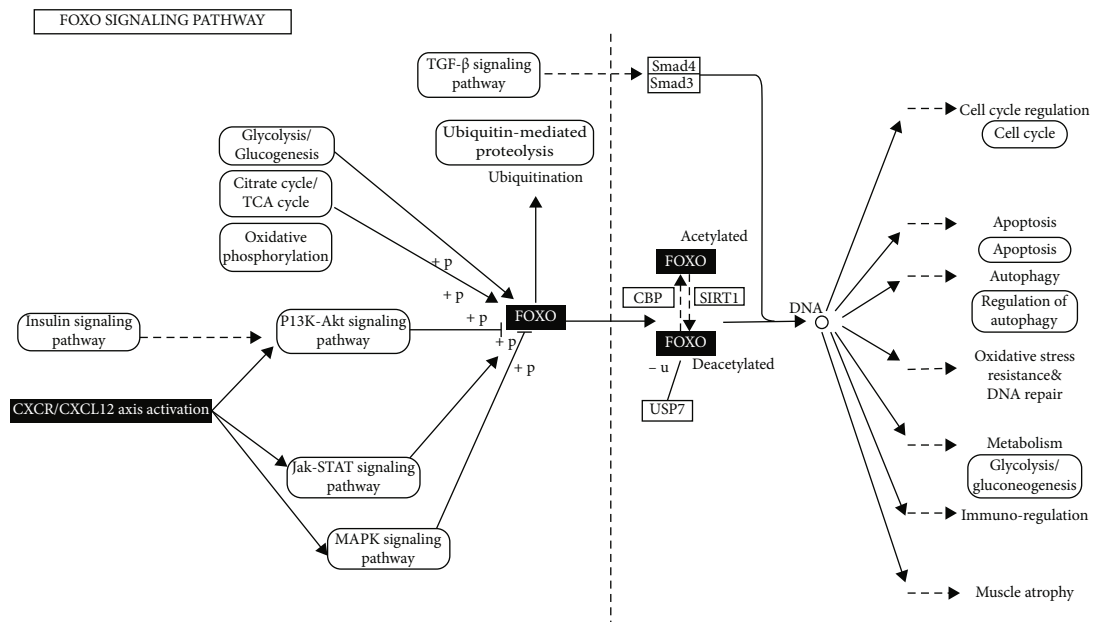
FIGURE 6: The forkhead box O (FOXO) protein family regulates the expression of genes in cellular physiological events including apoptosis, tumor angiogenesis, glucose metabolism, oxidative stress resistance, and DNA damage repair. PI3K-Akt signaling pathway is activated in response to CXCR4/CXCL12 activation. Then, FOXO proteins are phosphorylation by the serine/threonine kinase (AKT)/protein kinase B (PKB). Phosphorylated FOXOs result in the export of FOXOs from the nucleus to the cytoplasm, thereby decreasing expression of FOXO target genes. Other posttranslational modifications of FOXO include methylation, acetylation, ubiquitylation, and glycosylation.

PTEN/AKT/mTORC1 [35–37], MYC [38], Wnt [39], MAPK [40], and Hippo pathway [41]. Rinks et al. [42] reduced cellular cholesterol by blocking the high-density lipoprotein nanoparticles (HDL NP), which can also block the enhanced BCR signaling. In their study, they achieved both cellular cholesterol reduction and apoptosis in resistant ABC DLBCL cell lines by using ibrutinib and the spleen tyrosine kinase inhibitor together with HDL NP. Thus, some new cholesterol metabolites have recently become promising target drugs for cancer treatment [43–45]. In another study, metformin, a drug that can enhance insulin sensitivity, was identified to be associated with improved response rate and PFS in diabetic patients and is a possible therapeutic drug against DLBCL [46]. These results illustrate that reduction of cellular cholesterol or restoration of insulin sensitivity in lymphoma is a new method to induce tumor cell apoptosis. Our combined GSEA results indicate that cholesterol metabolism and insulin resistance may regulate complex signaling pathways and antitumor immunity and play important roles in high CXCR4 expression DLBCL. We hypothesize that CXCR4 antagonists may simultaneously inhibit MAPK, PI3k/AKT, and mTOR signaling pathway, inhibit cholesterol metabolism, and correct insulin resistance, which may exert a stronger inhibitory effect on the BCR signaling pathway.

Our GSEA results showed that genes from DLBCL patients with high CXCR4 expression are enriched in the forkhead box O- (FOXO-) mediated transcription of cell cycle genes. KOBAS analysis showed increased hub genes associated with the FOXO signaling pathway. FOXOs are tumor suppressors and can be used as key regulators of cell biology [47]. FOXO3a belongs to this family and functions as a trigger for apoptosis through the expression of genes necessary for cell death, and its inactivation is essential for the proliferation of immune cells. According to the study results of Kapoor et al. [48], Ibrutinib-resistant DLBCL (IB-R) cell lines showed downregulation of FOXO3a and PTEN levels in the nuclei and activation of AKT signaling. Therefore, they used a PI3K inhibitor and AKT inhibitor (idelalisib and MK2206) in IB-R cells, which resulted in increased ibrutinib-induced apoptosis. The drug selinexor (an exportin 1 inhibitor) together with ibrutinib can also increase the nuclear abundance of FOXO3a and PTEN in IB-R cells, leading to the restoration of ibrutinib-induced apoptosis. Our hub gene analysis revealed the coexpression of CXCR4 and hnRNPA2B1, which was confirmed by the (TIMER) gene correlation analysis. HnRNPA2B1 is involved in carcinogenesis by interacting with several proteins. One study found that it promotes the survival of tumor cells by preventing the activation of p53 [49]. In another study by Pan et al., CXCR4 was coimmunoprecipated with cyclophilin A (CyPA). Stimulation of CXCR4 induces CyPA phosphorylation and nuclear translocation. CyPA formed a complex with heterogeneous nuclear ribonucleoprotein (hnRNP) A2, which underwent nuclear export in response to the activation of CXCR4 and was blocked by RNAi of CyPA. Overall, these findings demonstrate that the CXCR4 antagonist exerts both effects on BCR signaling and nuclear export, restores the function of FOXO3a (Figure 6) and PTEN, reduces the nuclear export of hnRNPA2, and overcomes acquired resistance to BTK inhibitor in DLBCL patients.

According to our cell viability test, WZ811 suppressed the cell viability of both ABC-DLBCL (OCI-Ly3) and GCB-DLBCL (SU-DHL4), which confirmed the results of

our bioinformatics analysis (Figure 5). Currently, there are a rising number of clinical trials using CXCR4 antagonists for treating different malignant diseases [50]. One phase I study (NCT00903968) enrolled relapse/refractory multiple myeloma (RRMM). The study drugs were bortezomib (1.3 mg/m^2) and CXCR4 antagonist (the maximal-tolerated dose 0.32 mg/kg). Results of this clinical trial indicated that combination of these two drugs is safe and effective in RRMM. A phase Ib/II study also aimed to determine the safety and tolerability of the anti-CXCR4 antibody (ulocuplumab), alone and in combination with lenalidomide and dexamethasone, or with bortezomib and dexamethasone in patients with RRMM. This study showed that ulocuplumab is safe with acceptable adverse events and leads to a high response rate in combination with lenalidomide and dexamethasone in patients with RRMM. These results suggest that CXCR4 inhibitors are promising antimyeloma drugs. However, few clinical trials have been conducted on DLBCL; so, there is a potential for further exploration in clinical trials.

Certain limitations existed in our study. For example, there were a small number of verification samples in this study. Additionally, we simply divided the expression level of CXCR4 into high and low groups according to the median CXCR4 expression level and used negative and positive in the immunohistochemical stains. However, choosing the best immunohistochemical cutoff value may help us more sensitively and specifically identify high-risk DLBCL patients with the positive CXCR4 expression. Also, we used FFPE samples for qPCR due to lacking of fresh biopsy specimen, which may reduce the accuracy of experimental results. Limited variety of cell lines was also the shortcoming of our experiment. We hope to make up for the defects of these experiments in the future.

5. Conclusion

Overall, our study utilized a comprehensive analysis with experimental validation to imply the therapeutic significance of CXCR4 as a potential target in DLBCL, which may pave the way for precision therapy and translational medicine in the prognosis and treatment of DLBCL in the future.

Abbreviations

EZH2: Enhancer of zeste homolog 2
PI3K: Phosphatidylinositol-3-kinase
mTOR: Mammalian target of rapamycin
CXCR4: CXC chemokinereceptor 4
TCGA: The Cancer Genome Atlas
GEO: Gene Expression Omnibus
GSEA: Gene set enrichment analysis
PPI: Protein-protein interaction
TIMER: Tumor Immune Estimate Resource
ICI: Immune cell infiltration.

Data Availability

The data used to support the findings of this study are included within the article.

Ethical Approval

This study was approved by the ethics committee of the Zhongshan Hospital, Fudan University (B2021-025R), and written informed consent was signed by each participant.

Consent

Written consent was obtained from all patients.

Conflicts of Interest

The authors declare no conflicting interests.

Authors' Contributions

LP and ZYA contributed to the study design. ZYA and YX contributed to the drafting of the article. ZYA, YX, YJM, and RYH contributed to data collection. YJM contributed to immunohistochemistry evaluation. ZYA and YX contributed to the bioinformatics analysis. All authors reviewed and approved the final manuscript.

Acknowledgments

Supplementary Materials

Supplementary Tables. Table S1: list of antibodies. Table S2: results of gene set enrichment analysis (c2.all.v7.2.symbols.gmt). Supplementary Figure. Figure S1: relation between CXCR4 expression and macrophage M1 infiltration.Low CXCR4 expression group harbored a higher level of M1 macrophage infiltration ($P < 0.001$). (Supplementary Materials)

References

[1] L. H. Sehn and G. Salles, "Diffuse large B-cell lymphoma," The New England Journal of Medicine, vol. 384, no. 9, pp. 842–858, 2021.

[2] L. Fan, L. Li, Y. Zhou, and J. Li, "Rituximab-based therapy in newly diagnosed diffuse large B-cell lymphoma patients: individualized risk-adapted therapy approach using molecular subtypes," Journal of Hematology, vol. 6, no. 2-3, pp. 33–43, 2017.

[3] J. P. Leonard, K. Kolibaba, J. A. Reeves et al., "Randomized phase 2 open-label study of R-CHOP +/- bortezomib in patients (Pts) with untreated non-germinal center B-cell-like (Non-GCB) subtype diffuse large cell lymphoma (DLBCL): results from the pyramid trial (NCT00931918)," Blood, vol. 126, no. 23, p. 811, 2015.

[4] F. Offner, O. Samoilova, E. Osmanov et al., "Frontline rituximab, cyclophosphamide, doxorubicin, and prednisone with

bortezomib (VR-CAP) or vincristine (R-CHOP) for non-GCB DLBCL," *Blood*, vol. 126, no. 16, pp. 1893–1901, 2015.

[5] J. Vandercappellen, J. Van Damme, and S. Struyf, "The role of CXC chemokines and their receptors in cancer," *Cancer Letters*, vol. 267, no. 2, pp. 226–244, 2008.

[6] T. Pozzobon, G. Goldoni, A. Viola, and B. Molon, "CXCR4 signaling in health and disease," *Immunology Letters*, vol. 177, pp. 6–15, 2016.

[7] Y. Qin, F. Wang, H. Ni et al., "Cancer-associated fibroblasts in gastric cancer affect malignant progression via the CXCL12-CXCR4 axis," *Journal of Cancer*, vol. 12, no. 10, pp. 3011–3023, 2021.

[8] F. Yang, Y. Takagaki, Y. Yoshitomi et al., "Inhibition of dipeptidyl peptidase-4 accelerates epithelial-mesenchymal transition and breast cancer metastasis via the CXCL12/CXCR4/mTOR axis," *Cancer Research*, vol. 79, no. 4, pp. 735–746, 2019.

[9] O. Wald, "CXCR4 based therapeutics for non-small cell lung cancer (NSCLC)," *Journal of Clinical Medicine*, vol. 7, no. 10, p. 303, 2018.

[10] B. Bockorny, V. Semenisty, T. Macarulla et al., "BL-8040, a CXCR4 antagonist, in combination with pembrolizumab and chemotherapy for pancreatic cancer: the COMBAT trial," *Nature Medicine*, vol. 26, no. 6, pp. 878–885, 2020.

[11] A. Figueras, E. Alsina-Sanchís, A. Lahiguera et al., "A role for CXCR4 in peritoneal and hematogenous ovarian cancer dissemination," *Molecular Cancer Therapeutics*, vol. 17, no. 2, pp. 532–543, 2018.

[12] H. Minami, K. Nagaharu, Y. Nakamori et al., "CXCL12-CXCR4 Axis is required for contact-mediated human B lymphoid and plasmacytoid dendritic cell differentiation but not T lymphoid generation," *Journal of Immunology*, vol. 199, no. 7, pp. 2343–2355, 2017.

[13] A. Peled, S. Klein, K. Beider, J. A. Burger, and M. Abraham, "Role of CXCL12 and CXCR4 in the pathogenesis of hematological malignancies," *Cytokine*, vol. 109, pp. 11–16, 2018.

[14] Y. Hu, M. Gale, J. Shields et al., "Enhancement of the antitumor activity of therapeutic monoclonal antibodies by CXCR4 antagonists," *Leukemia & Lymphoma*, vol. 53, no. 1, pp. 130–138, 2012.

[15] J. Chen, Z. Y. Xu-Monette, L. Deng et al., "Dysregulated CXCR4 expression promotes lymphoma cell survival and independently predicts disease progression in germinal center B-cell-like diffuse large B-cell lymphoma," *Oncotarget*, vol. 6, no. 8, pp. 5597–5614, 2015.

[16] H. C. Shin, J. Seo, B. W. Kang et al., "Clinical significance of nuclear factor κB and chemokine receptor CXCR4 expression in patients with diffuse large B-cell lymphoma who received rituximab-based therapy," *The Korean Journal of Internal Medicine*, vol. 29, no. 6, pp. 785–792, 2014.

[17] A. A. Alizadeh, M. B. Eisen, R. E. Davis et al., "Distinct types of diffuse large B-cell lymphoma identified by gene expression profiling," *Nature*, vol. 403, no. 6769, pp. 503–511, 2000.

[18] G. Gutiérrez-García, T. Cardesa-Salzmann, F. Climent et al., "Gene-expression profiling and not immunophenotypic algorithms predicts prognosis in patients with diffuse large B-cell lymphoma treated with immunochemotherapy," *Blood*, vol. 117, no. 18, pp. 4836–4843, 2011.

[19] S. B. Peng, V. Peek, Y. Zhai et al., "Akt activation, but not extracellular signal-regulated kinase activation, is required for SDF-1α/CXCR4–mediated migration of epitheloid carci-noma cells," *Molecular Cancer Research*, vol. 3, no. 4, pp. 227–236, 2005.

[20] Y. Han, T. He, D. R. Huang, C. A. Pardo, and R. M. Ransohoff, "TNF-alpha mediates SDF-1 alpha-induced NF-kappa B activation and cytotoxic effects in primary astrocytes," *The Journal of Clinical Investigation*, vol. 108, no. 3, pp. 425–435, 2001.

[21] T. Yuan, F. Zhang, X. Zhou et al., "Inhibition of the PI3K/AKT signaling pathway sensitizes diffuse large B-cell lymphoma cells to treatment with proteasome inhibitors via suppression of BAG3," *Oncology Letters*, vol. 17, no. 4, pp. 3719–3726, 2019.

[22] B. An, S. Zhu, T. Li et al., "A dual TLR7/TLR9 inhibitor HJ901 inhibits ABC-DLBCL expressing the MyD88 L265P mutation," *Frontiers in Cell and Development Biology*, vol. 8, p. 262, 2020.

[23] Z. Li, F. Yu, W. Ye et al., "Clinical features and prognostic significance of NOTCH1 mutations in diffuse large B-cell lymphoma," *Frontiers in Oncology*, vol. 11, p. 746577, 2021.

[24] M. Cojoc, C. Peitzsch, F. Trautmann, L. Polishchuk, G. D. Telegeev, and A. Dubrovska, "Emerging targets in cancer management: role of the CXCL12/CXCR4 axis," *Oncotargets and Therapy*, vol. 6, pp. 1347–1361, 2013.

[25] J. M. Busillo and J. L. Benovic, "Regulation of CXCR4 signaling," *Biochimica et Biophysica Acta*, vol. 1768, no. 4, pp. 952–963, 2007.

[26] A. Majchrzak, M. Witkowska, and P. Smolewski, "Inhibition of the PI3K/Akt/mTOR signaling pathway in diffuse large B-cell lymphoma: current knowledge and clinical significance," *Molecules*, vol. 19, no. 9, pp. 14304–14315, 2014.

[27] Z. Z. Xu, J. K. Shen, S. Q. Zhao, and J. M. Li, "Clinical significance of chemokine receptor CXCR4 and mammalian target of rapamycin (mTOR) expression in patients with diffuse large B-cell lymphoma," *Leukemia & Lymphoma*, vol. 59, no. 6, pp. 1451–1460, 2018.

[28] Y. Wang, M. Zhang, H. Xu et al., "Discovery and validation of the tumor-suppressive function of long noncoding RNA PANDA in human diffuse large B-cell lymphoma through the inactivation of MAPK/ERK signaling pathway," *Oncotarget*, vol. 8, no. 42, pp. 72182–72196, 2017.

[29] Y. Xu, W. Sun, and F. Li, "De novo CD5+ diffuse large B-cell lymphoma: biology, mechanism, and treatment advances," *Clinical Lymphoma, Myeloma & Leukemia*, vol. 20, no. 10, pp. e782–e790, 2020.

[30] M. F. Breinholt, D. Oliveira, T. W. Klausen et al., "High-grade B-cell lymphomas with MYC and BCL2 translocations lack tumor-associated macrophages and PD-L1 expression: a possible noninflamed subgroup," *Hematological Oncology*, vol. 39, no. 3, pp. 284–292, 2021.

[31] S. Zhou, H. Lu, and M. Xiong, "Identifying immune cell infiltration and effective diagnostic biomarkers in rheumatoid arthritis by bioinformatics analysis," *Frontiers in Immunology*, vol. 12, p. 726747, 2021.

[32] C. Chang, Y. P. Chen, L. J. Medeiros, T. Y. Chen, and K. C. Chang, "Higher infiltration of intratumoral CD25+ FOXP3+ lymphocytes correlates with a favorable prognosis in patients with diffuse large B-cell lymphoma," *Leukemia & Lymphoma*, vol. 62, no. 1, pp. 76–85, 2021.

[33] M. Autio, S. K. Leivonen, O. Brück et al., "Immune cell constitution in the tumor microenvironment predicts the outcome in diffuse large B-cell lymphoma," *Haematologica*, vol. 106, no. 3, pp. 718–729, 2021.

[34] S. Merdan, K. Subramanian, T. Ayer et al., "Gene expression profiling-based risk prediction and profiles of immune infiltration in diffuse large B-cell lymphoma," *Blood Cancer Journal*, vol. 11, no. 1, p. 2, 2021.

[35] B. M. Castellano, A. M. Thelen, O. Moldavski et al., "Lysosomal cholesterol activates mTORC1 via an SLC38A9-Niemann-pick C1 signaling complex," *Science*, vol. 355, no. 6331, pp. 1306–1311, 2017.

[36] W. Eid, K. Dauner, K. C. Courtney et al., "mTORC1 activates SREBP-2 by suppressing cholesterol trafficking to lysosomes in mammalian cells," *Proceedings of the National Academy of Sciences of the United States of America*, vol. 114, no. 30, pp. 7999–8004, 2017.

[37] T. R. Peterson, S. S. Sengupta, T. E. Harris et al., "mTOR complex 1 regulates lipin 1 localization to control the SREBP pathway," *Cell*, vol. 146, no. 3, pp. 408–420, 2011.

[38] F. Yang, J. Kou, Z. Liu, W. Li, and W. Du, "MYC enhances cholesterol biosynthesis and supports cell proliferation through SQLE," *Frontiers in Cell and Development Biology*, vol. 9, p. 655889, 2021.

[39] R. Sheng, H. Kim, H. Lee et al., "Cholesterol selectively activates canonical Wnt signalling over non- canonical Wnt signalling," *Nature Communications*, vol. 5, no. 1, p. 4393, 2014.

[40] C. Wang, P. Li, J. Xuan et al., "Cholesterol enhances colorectal cancer progression via ROS elevation and MAPK signaling pathway activation," *Cellular Physiology and Biochemistry*, vol. 42, no. 2, pp. 729–742, 2017.

[41] X. Wang, B. Cai, X. Yang et al., "Cholesterol stabilizes TAZ in hepatocytes to promote experimental non- alcoholic steatohepatitis," *Cell Metabolism*, vol. 31, no. 5, pp. 969–986, 2020, e967.

[42] J. S. Rink, S. Yang, O. Cen et al., "Rational targeting of cellular cholesterol in diffuse large B-cell lymphoma (DLBCL) enabled by functional lipoprotein nanoparticles: a therapeutic strategy dependent on cell of origin," *Molecular Pharmaceutics*, vol. 14, no. 11, pp. 4042–4051, 2017.

[43] Y. Jiang, A. Sun, Y. Zhao et al., "Proteomics identifies new therapeutic targets of early-stage hepatocellular carcinoma," *Nature*, vol. 567, no. 7747, pp. 257–261, 2019.

[44] D. Liu, C. C. Wong, L. Fu et al., "Squalene epoxidase drives NAFLD-induced hepatocellular carcinoma and is a pharmaceutical target," *Science Translational Medicine*, vol. 10, no. 437, p. eaap9840, 2018.

[45] X. Gong, H. Qian, X. Zhou et al., "Structural insights into the Niemann-Pick C1 (NPC1)-mediated cholesterol transfer and Ebola infection," *Cell*, vol. 165, no. 6, pp. 1467–1478, 2016.

[46] X. N. Jiang, Y. Zhang, W. G. Wang, D. Sheng, X. Y. Zhou, and X. Q. Li, "Alteration of cholesterol metabolism by metformin is associated with improved outcome in type II diabetic patients with diffuse large B-cell lymphoma," *Frontiers in Oncology*, vol. 11, p. 608238, 2021.

[47] M. Farhan, H. Wang, U. Gaur, P. J. Little, J. Xu, and W. Zheng, "FOXO signaling pathways as therapeutic targets in cancer," *International Journal of Biological Sciences*, vol. 13, no. 7, pp. 815–827, 2017.

[48] I. Kapoor, Y. Li, A. Sharma et al., "Resistance to BTK inhibition by ibrutinib can be overcome by preventing FOXO3a nuclear export and PI3K/AKT activation in B-cell lymphoid malignancies," *Cell Death & Disease*, vol. 10, no. 12, p. 924, 2019.

[49] H. Pan, C. Luo, R. Li et al., "Cyclophilin A is required for CXCR4-mediated nuclear export of heterogeneous nuclear ribonucleoprotein A2, activation and nuclear translocation of ERK1/2, and chemotactic cell migration," *The Journal of Biological Chemistry*, vol. 283, no. 1, pp. 623–637, 2008.

[50] C. Tomowiak, S. Poulain, C. Herbaux et al., "Obinutuzumab and idelalisib in symptomatic patients with relapsed/refractory Waldenström macroglobulinemia," *Blood Advances*, vol. 5, no. 9, pp. 2438–2446, 2021.